

Article

Saturated Resin Ectopic Regeneration by Non-Thermal Dielectric Barrier Discharge Plasma

Chunjing Hao , Zehua Xiao, Di Xu, Chengbo Zhang, Jian Qiu and Kefu Liu *

Department of Light Sources & Illuminating Engineering, Fudan University, Shanghai 200433, China; 17110720032@fudan.edu.cn (C.H.); zhxiao14@fudan.edu.cn (Z.X.); 15210720020@fudan.edu.cn (D.X.); 13110720012@fudan.edu.cn (C.Z.); jqiu@fudan.edu.cn (J.Q.)

* Correspondence: kfliu@fudan.edu.cn; Tel.: +86-21-5566-5184

Received: 26 October 2017; Accepted: 22 November 2017; Published: 27 November 2017

Abstract: Textile dyes are some of the most refractory organic compounds in the environment due to their complex and various structure. An integrated resin adsorption/Dielectric Barrier Discharge (DBD) plasma regeneration was proposed to treat the indigo carmine solution. It is the first time to report ectopic regeneration of the saturated resins by non-thermal Dielectric Barrier Discharge. The adsorption/desorption efficiency, surface functional groups, structural properties, regeneration efficiency, and the intermediate products between gas and liquid phase before and after treatment were investigated. The results showed that DBD plasma could maintain the efficient adsorption performance of resins while degrading the indigo carmine adsorbed by resins. The degradation rate of indigo carmine reached 88% and the regeneration efficiency (RE) can be maintained above 85% after multi-successive regeneration cycles. The indigo carmine contaminants were decomposed by a variety of reactive radicals leading to fracture of exocyclic C=C bond, which could cause decoloration of dye solution. Based on above results, a possible degradation pathway for the indigo carmine by resin adsorption/DBD plasma treatment was proposed.

Keywords: indigo carmine; resin; Dielectric Barrier Discharge; adsorption; regeneration

1. Introduction

Industrial production processes, especially in printing and dyeing manufacturing, generate large quantities of refractory wastewater every year [1–3]. Organic chemical dyestuffs are applied as coloring material in textile industry, and are hard to degrade in normal ways, such as adsorption [4,5], biological [6], and chemical methods [7,8]. These methods have many disadvantages. On the one hand, in biological treatment, is difficult to cultivate suitable active species. On the other hand, chemical disposal often brings the problem of secondary pollution. In addition, the physical adsorption method is only a phase transfer of contaminants, and adsorbents are usually by chemical regeneration, resulting in secondary contamination of chemical reagents. Hence, systems of advanced oxidation processes (AOPs) with conventional approaches are integrated for the decomposition of organic dye contaminants, such as Fenton oxidation process ($\text{H}_2\text{O}_2 + \text{Fe}^{2+}$) [9], ozone and UV ($\text{O}_3 + \text{UV}$), photocatalytic oxidation ($\text{TiO}_2 + \text{UV}$), and Non-thermal plasma (NTP) [10–12]. These methods are mainly based on the strong oxidative properties of hydroxyl radical and degradation of organic molecules. The history of Dielectric Barrier Discharge can be traced back to 1857 [13]. In 1987, Sidney first presented the technique of high voltage pulsed discharge to dispose of sewage [14]. After that, many research teams have studied the applications in various areas [15–17]. DBD plasma is widely used in the environmental protection because it produces a large number of high energy electrons, intense UV radiation, and a variety of chemical free radicals (e.g., hydroxyl radical, high energy oxygen atoms, etc.), which can rapidly react with most of the bio-refractory organic pollutants. Nevertheless,

DBD plasma technology alone needs higher energy consumption, and wastewater quality factors, such as concentration, conductivity, and pH value, greatly affect the degradation effect. In particular, relatively low concentration and Chemical Oxygen Demand (COD) may greatly waste discharge energy, and more energy probably heats the wastewater solution. Hence, one of the most promising technologies, combining adsorption and DBD plasma to degrade pollutants, was introduced. Research on highly concentrated pollutants and regeneration for saturated adsorbent has been reported [18,19]. At present, the adsorbents applied in the wastewater treatment are Granular Activated Carbon (GAC), zeolite, activated alumina, etc. [20,21]. However, although Activated Carbon (AC) has been widely used in the industry, the adsorption performance of saturated AC greatly decreases after multiple regeneration. Moreover, the regeneration of AC is difficult, for example the use of heating regeneration method resulting in high carbon loss rate, or the use of pharmaceutical regeneration method resulting in high costs and secondary pollution. AC is also conductive, which is not conducive to DBD plasma discharge [22]. Based on some related literature [23–25], resin has strong adsorption properties, and can keep strong ability to absorb contaminants through repeated regeneration. The general regenerative method is eluted by mixed solution, which can lead to chemical secondary pollution [26]. Unlike the general methods, DBD discharge regeneration can achieve double effect, in which concentrated pollutants onto resins are decomposed and saturated resins are regenerated to restore the adsorption performance. At present, no literature has mentioned the study on regeneration of resin by plasma. In this article, we conducted an in-depth study that confirmed the combination of resin adsorption and DBD regeneration process can greatly improve the degradation efficiency of pollutants and reduce operating costs.

In this paper, a flat-plate reactor to investigate a facile wastewater treatment technique was designed. There are five aspects researched: (1) the adsorption behavior of resin about indigo carmine solution; (2) the regeneration efficiency for multiple cycles; (3) the functional groups and structure properties of resin before and after DBD plasma treatment; (4) the analysis of intermediate products in gas and liquid phase; and (5) a possible degradation pathway of indigo carmine contaminants by resin adsorption/DBD plasma discharge treatment system. The technique of integrated resin adsorption/DBD plasma regeneration method has very broad prospects in the field of environment protection.

2. Results

Degradation Pathway Process

The possible reaction pathway for the degradation of indigo carmine solution by adsorption/DBD plasma regeneration system was proposed (Figure 1). The pathway included all of the detected intermediates and showed the active radicals as oxidant, especially the hydroxyl radical formed in the DBD discharge process. Other weak oxidants were also possible, such as H_2O_2 and HO_2 . According to the LC-MS analysis results, isatin 5-sulfonic acid (m/z 226) was the main aromatic product produced when a hydrogen radical attacked the C=C bond of indigo carmine. Isatin 5-sulfonic acid then lost SO_4^{2-} and converted to isatin. Further oxidation of the intermediate products led to a mixture of carboxylic acid and amine. Finally, those carboxylic acid and amine were degraded to inorganic molecule, including of carbon dioxide, ammonium, nitrate, etc.

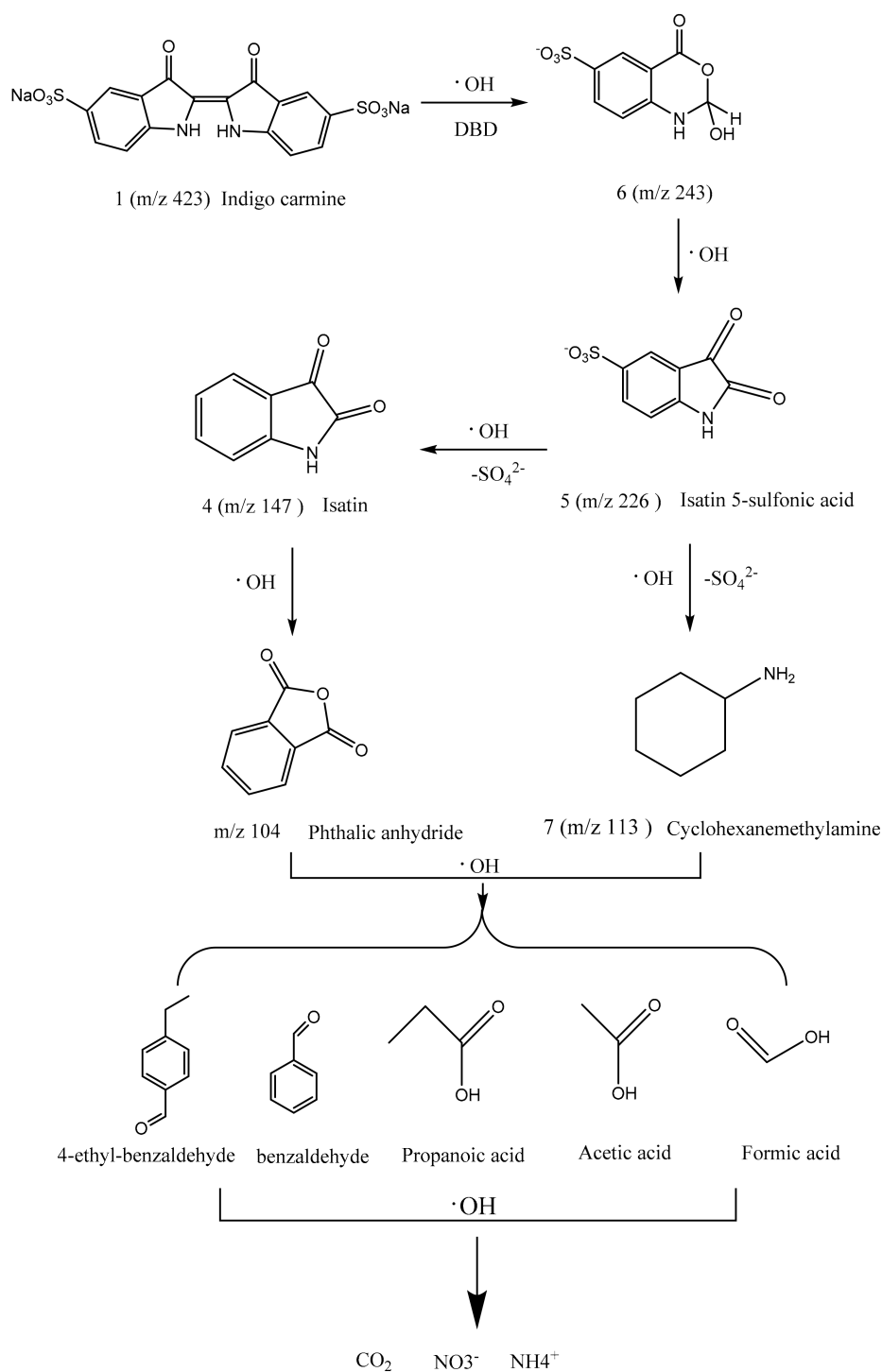


Figure 1. Degradation pathway of indigo carmine in an integrated resin adsorption/DBD plasma.

3. Discussion

3.1. Effect of Regeneration on Adsorption Capacity and Kinetics of Resin

By comparing the adsorption isotherms of virgin resin with a series of DBD regenerated resins, the effect of DBD plasma on the adsorption capacity was analyzed. Figure 2 depicts the adsorption isotherms of indigo carmine on virgin and series of adsorption/DBD regenerated resins. It was

observed that the adsorption capacity of regenerated resin is reduced, and, as the regeneration cycle progresses, the q_e value of the resin samples decreased.

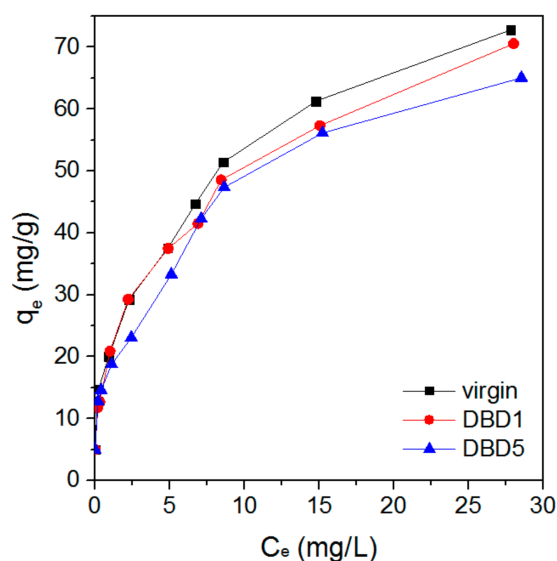


Figure 2. Adsorption isotherms of indigo carmine on virgin and different saturated/DBD regeneration resins.

On the other hand, the adsorption type of indigo carmine onto resin samples after DBD plasma treatment was also studied. Generally, the Freundlich model was a kind of adsorption isotherm model, which was generally expressed by Freundlich equation (see, e.g., [27]):

$$q_e = K_F C_e^{1/n}, \quad (1)$$

where q_e is the amount of adsorption equilibrium state, mg/g; C_e is the concentration of equilibrium solution, mg/L; K_F (L/g) is the Freundlich parameter interaction with adsorption and adsorption capacity; and the exponential term of $1/n$ (dimensionless) is related to the adsorption force. $\ln q_e$ and $\ln C_e$ plotted in a straight line from the slope and intercept of the straight line were the values of $1/n$ and $\ln K_F$, respectively. The fitting curve of the linear correlation coefficient was R^2 . The above three constants are listed in Table 1. The results showed that all isotherms fitted well to the Freundlich equation, which indicated that regeneration process did not seem to alter adsorption processes. All $1/n$ values were less than 1, which indicated further adsorption of indigo carmine onto resins. The adsorption isotherms of indigo carmine onto resins confirmed this phenomenon (Figure 2).

Table 1. Freundlich constants for adsorption of indigo carmine onto resin.

Sample	K_F (L/g)	$1/n$	R^2
Virgin	2.31	0.33	0.989
DBD1	2.39	0.30	0.979
DBD5	2.29	0.30	0.989

3.2. Effect of Regeneration on the Regeneration Efficiency

The residual concentration changes of indigo carmine were analyzed on virgin and DBD regenerated resins (Figure 3). Five DBD treated cycle experiments were conducted. The first to fifth DBD plasma regeneration experiments were abbreviated as DBD1, DBD2, DBD3, DBD4, and DBD5, respectively. There was only a little change in adsorption rate for DBD regenerated resins, demonstrating that adsorption rate almost kept the same level after five cycles of regeneration. Hence,

the DBD regeneration efficiency could directly reveal the impact of DBD discharge process, which was calculated using the following Equation (2):

$$RE = \frac{q_r}{q_v} \times 100\%, \quad (2)$$

where q_v and q_r are the amounts of adsorption equilibrium state of indigo carmine on virgin and regenerated resins, respectively (mg/g).

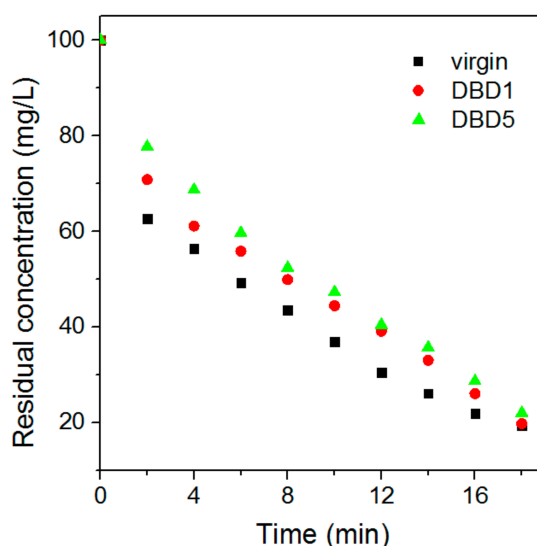


Figure 3. Residual concentration changes of indigo carmine solutions by virgin and different saturated/DBD regeneration resins.

All regeneration efficiencies of this process by series of regeneration cycles are presented in Figure 4. The residual concentration of the indigo carmine solution adsorbed by the virgin and regenerated resin was basically achieved, which was less than 20%. At the same time, it was also observed that, as the number of regeneration cycles increased, the degradation efficiency remained almost unchanged, indicating that the structural properties of resins remained stable and DBD plasma did not cause serious damage to the active sites on the surface of resins (discussed below). As can be seen in Figure 4, the regeneration efficiency of the resin was maintained at 80% or more even after five regeneration cycles. The experimental setup was high voltage value of 18 kV, current of 4.32 A, frequency of 1 kHz, and the degradation rate of 86%. The energy efficiency of resin adsorption/DBD plasma treatment was 139.5 g/kWh, whereas the DBD plasma treating the same concentration of indigo carmine was 56.5 g/kWh, based on the previous work [2]. The energy efficiency of adsorption/DBD regeneration was greater than 2.5 times the DBD plasma system.

The UV-Vis spectra of the resin samples at each treatment cycle are shown in Figure 5. The peaks were caused by the residual indigo carmine and intermediates onto resins after DBD regeneration. The wavelengths of 610, 450, 280, and 250 nm onto regenerated resins were observed before and after treatment of the UV-Vis spectra. The wavelength of 610 nm was characteristic absorption peak of indigo carmine. Moreover, the chromophoric group and unsaturated bond of indigo carmine correspond to the wavelengths of 610 and 250 nm, respectively. The formula of the indigo carmine is shown in the inset of Figure 5, and the bond in the bracket is the chromophoric group. The absorption intensity of all of the peaks decreased through every regeneration cycles. These results showed that chromophoric and unsaturated bonds of indigo carmine were almost broken up, which illuminated that the saturated resin was regenerated sufficiently, maintaining great degradation efficiency after multiple successive discharge cycles, which is a promising technique.

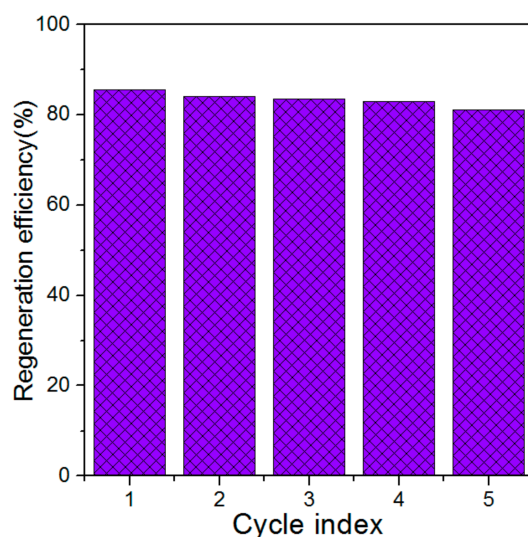


Figure 4. The regeneration efficiencies of resins after DBD plasma multiple cycles.

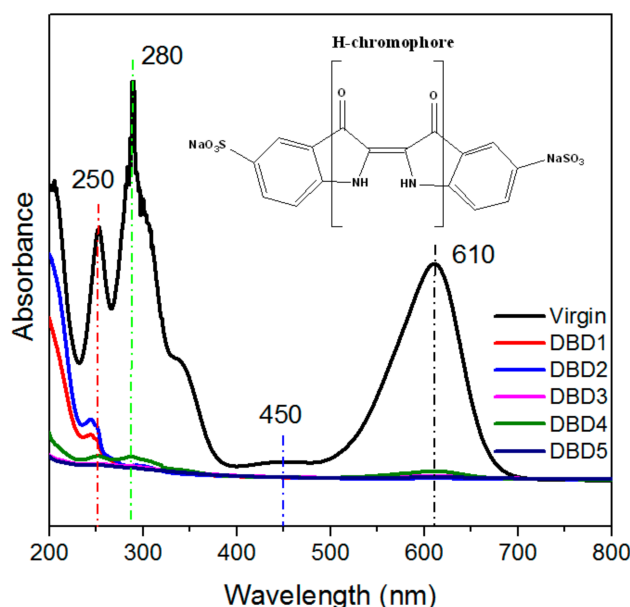


Figure 5. The UV-Vis spectra of virgin and DBD regeneration treatment resins.

3.3. Changes in the Structural Properties of Resins

The chemical bonds of the resin were characterized with FT-IR (fourier transform infrared spectroscopy) spectrometer. The FT-IR spectra of the three kinds of resins sample, containing virgin, saturated adsorbed resin, and adsorbed/DBD plasma regenerated resin, are depicted in Figure 6. The peaks at the wavelength of ~ 3420 , ~ 2940 , ~ 1650 , ~ 1450 , ~ 1100 , and ~ 680 cm^{-1} for all of the resin samples indicated that the resin surface functional groups were not destroyed. The broadening band around the main peak, ~ 3420 cm^{-1} , could be mainly caused by O-H stretching vibration peak in water [25]. The peak at ~ 3420 cm^{-1} was a multi-absorption peak, which was widened by overlapping with nitrogen hydrogen bond (N-H) and O-H stretching vibration peaks. The absorption peak at ~ 2940 cm^{-1} was mainly caused by porogen (polyethylene glycol), and residual organic liquid paraffin on the resin surface. The N-H bending vibration absorption peak corresponded to the position at ~ 1650 cm^{-1} . The band of 1450 cm^{-1} was primarily linked to the aromatic ring of C=C functional groups. At the peak of 1100 cm^{-1} , it was generally matched with C-O stretching in the lactate and ether

groups [28]. The adsorption intensity of the saturated adsorbed resins had enhanced compared with the virgin resin, which demonstrated clearly that adsorbed contaminants onto resins could increase the intense of hydrogen bond, double bond of carbon, and carbon oxygen bond. After the multiple regenerative cycles plasma treatment, the intensity of all the absorption peaks were decelerated compared with saturated resin, which was possible on account of the adsorbed indigo carmine onto resin achieved a certain degree of degradation. Note that the bond around 680 cm^{-1} attributed C-N bonds of indigo carmine were cleaved partially and indigo carmine was decomposed to some decolorized intermediates [29].

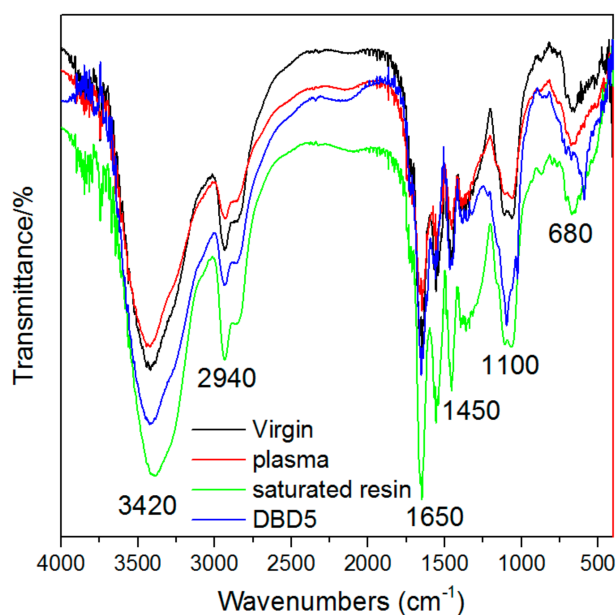


Figure 6. FT-IR spectra of the four kinds of virgin, plasma, saturated and DBD5 resins.

Apart from the analysis of functional groups, the structural characteristics of virgin, saturated, and DBD5 resins are listed in Table 2. The analysis showed that virgin and DBD5 resins exhibited similar specific surface area, total pore volume, pore size, and adsorption capacity. The analysis showed that DBD plasma regeneration process did not destroy the structure of resin. Therefore, the reason of the reduced performance of the saturated resin was that the adsorbed organic molecules occupied the adsorption site.

Table 2. Structural characteristics of virgin, saturated, and regenerated samples.

Sample	S_{BET} (m^2/g)	$V_{\text{Total pore}}$ (cm^3/g)	Pore Size (nm)	Adsorption Capacity (mg/g)
Virgin	163	0.3210	43.05	-
Saturated	74.6	0.1630	23.94	70.58
DBD5	157.8	0.299	46.33	65.06

3.4. Identification of Intermediates by GC-MS and LC-MS

As shown in Figure 7, the GC-MS (gas chromatography-mass spectrometer) analysis exhibited six peaks related to formic acid ($m/z = 29$) at $t_r = 1.6$ min, acetic acid ($m/z = 43$) at $t_r = 1.75$ min, benzaldehyde ($m/z = 105$) at $t_r = 3.17$ min, octamethyl-cyclotetrasiloxane ($m/z = 281$) at $t_r = 4.5$ min, 4-ethyl-benzaldehyde ($m/z = 134$) at $t_r = 5.63$ min, and phthalic anhydride ($m/z = 104$) at $t_r = 6.45$ min. The peak position was almost identical to a previous study [30]. Note that carboxylic acids came from the heterocyclic ring opening of isatin-5-sulfonic acid sodium salt dihydrate, which was been confirmed during DBD plasma degradation of indigo carmine. Aldehyde and acid anhydride could be

formed from the oxidation of their CO-NH-CO groups. Octamethyl was a kind of siloxane copolymer, which was probably formed when silica wool was heated. The cooperation of the plasma with the resin would still produce some intermediate products. The results are listed in Table 3.

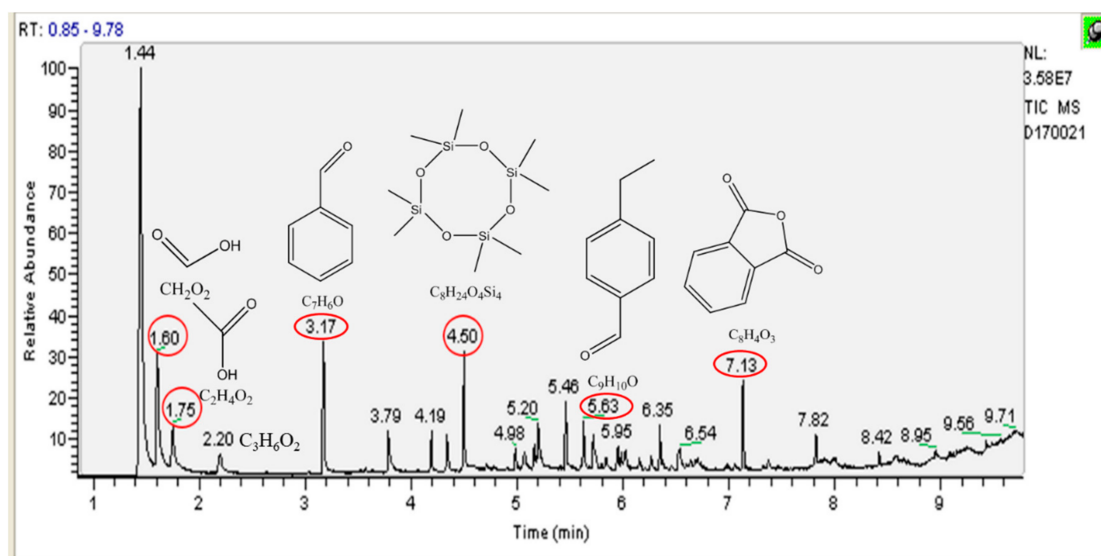


Figure 7. Total ion chromatogram of decomposed compositions by GC-MS analysis.

Table 3. Analysis of degradation products by GC-MS.

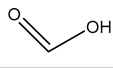
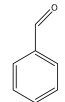
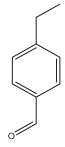
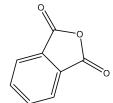
Compound	Structure	Molecular Formula	Retention Time (min)
Formic acid		CH ₂ O ₂	1.6
Acetic acid		C ₂ H ₄ O ₂	1.75
Propanoic acid		C ₃ H ₆ O ₂	2.2
Benzaldehyde		C ₇ H ₆ O	3.17
Octamethyl-cyclotetrasiloxane		C ₈ H ₂₄ O ₄ Si ₄	4.5
4-ethyl-benzaldehyde		C ₉ H ₁₀ O	5.63
Phthalic anhydride		C ₈ H ₄ O ₃	7.13

Figure 8 displays the LC-MS (liquid chromatography-mass spectrometer) analysis of the indigo carmine solution and the molecular formula of indigo carmine. Note that main charged anion of m/z

423 and its isotopic variants including m/z 423.9 ($m+1$) and 425 ($m+2$) well fitted those calculated for $C_{16}H_8N_2O_8S_2$. The anion of m/z 423 was detected as the primary species in dying solution.

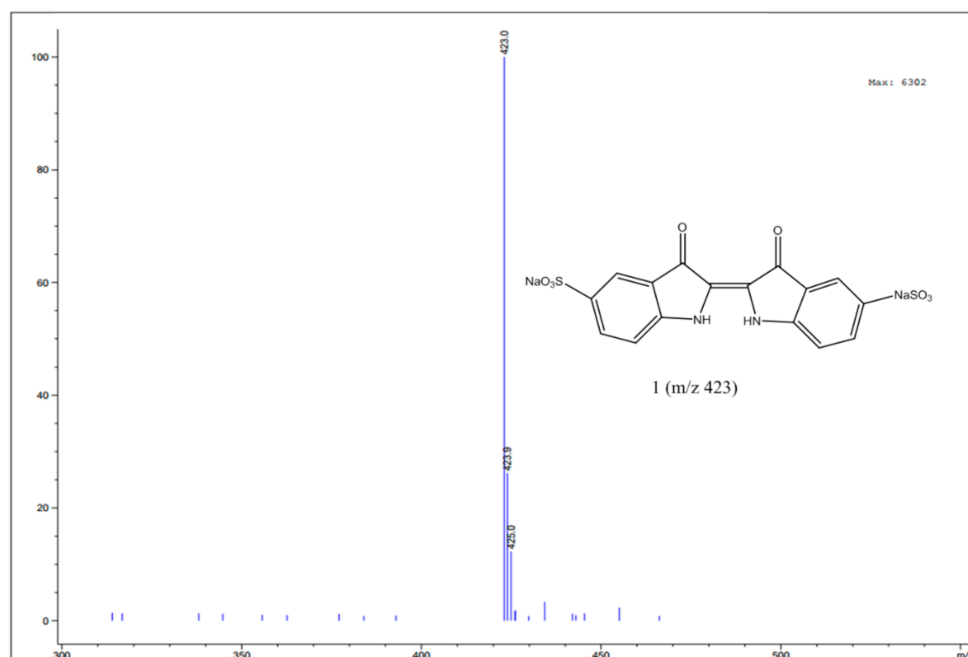


Figure 8. LC-MS analysis of initial indigo carmine solution.

The LC-MS analysis of the indigo carmine aqueous solution adsorbed by virgin resin and the molecular formula of the predominant component is shown in Figure 9. Whereas the anion of m/z 423 was not detected, ions of m/z 228.2, 229.3, 250.3, and 338.5 were clearly observed. Obviously, the components of m/z 228.2 ($m+1$) and m/z 229.3 ($m+2$) were isotopologs of isatin 5-sulfonic acid with molecular formula of $C_8H_5NO_5S$ [31]. The cation of m/z 250.3 was an isotopolog of 5-Isatinsulfonic acid sodium salt, which proved the fracture of $C=C$ bond. Based on these results, the continuous formation of intermediates adsorbed onto virgin resin had a much smaller π -electron conjugated system than the initial molecule, which could result in the indigo carmine solution decoloration, as experimentally observed. To analyze the residual pollutants on the surface of the plasma regenerated resin, LC-MS of indigo carmine solution adsorbed onto resin regenerated by DBD plasma and the molecular formula of the main byproducts are shown in Figure 10. The anion of m/z 226.1 is doubly charged, as evidenced by the presence of the ($M+1$) isotopologs of m/z 226. The $\Delta m/z$ for the doubly charged anions m/z 226.1 and 243.9 was 18 units, which indicated the latter molecule could be formed from the former via the incorporation of two hydroxyl groups. The anion of m/z 113.1 could probably be fitted with cyclohexylmethanamine with molecular formula of $C_7H_{15}N$. The peaks at other locations might be caused by residual surfactant on the surface of resin. Therefore, the formation of these intermediate products in aqueous solution was owing to fracture of the chromophoric $C=C$ group and incorporation of oxygen atoms, hydroxyl groups, etc. Hence, the analysis of indigo carmine degraded by DBD plasma treatment by LC-MS allowed us to detect unknown byproducts and analyze the degradation pathway in the reaction. Soem of the intermediates in aqueous solution by resin adsorption/DBD plasma regeneration are listed in Table 4.

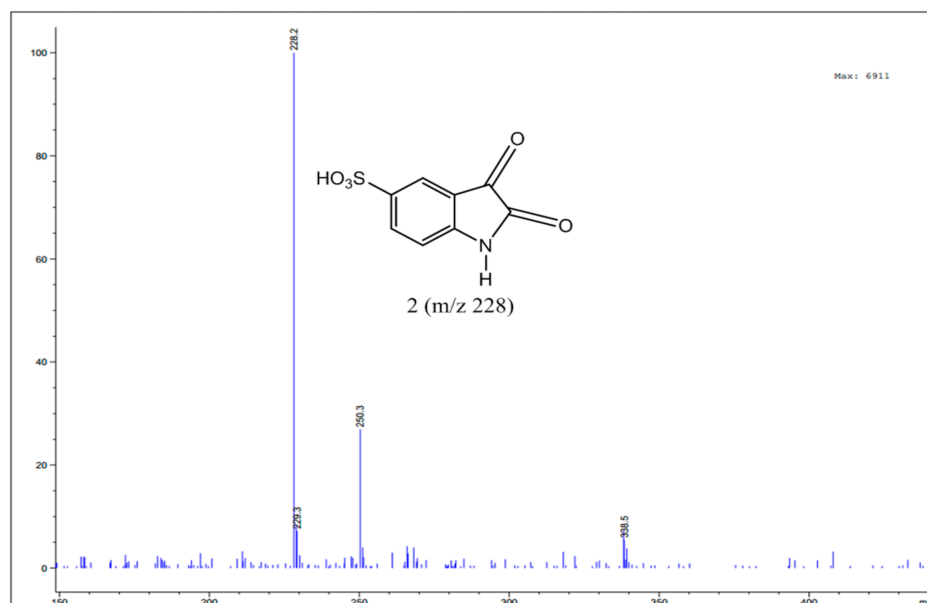


Figure 9. LC-MS analysis of indigo carmine solution adsorbed by virgin resin sample.

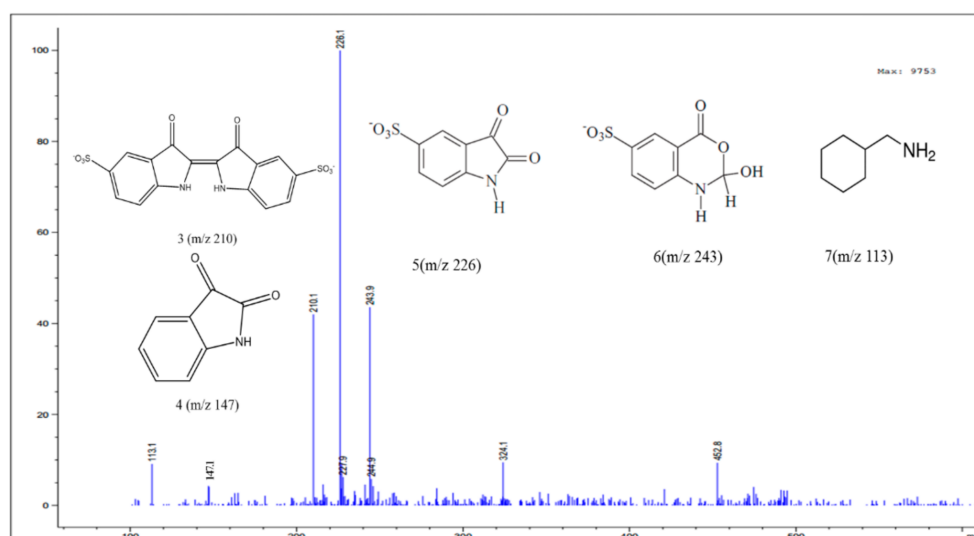


Figure 10. LC-MS analysis of indigo carmine solution adsorbed by plasma regenerated sample.

Table 4. Analysis of degradation products by LC-MS.

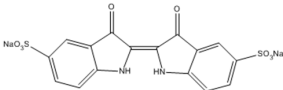
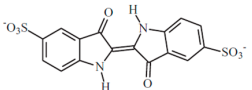
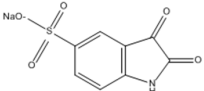
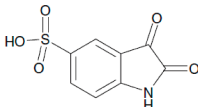
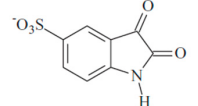
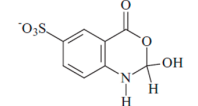
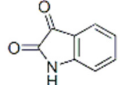
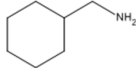
Compound	Structure	Molecular Formula	MS Fragments (<i>m/z</i>)
Indigo carmine		$C_{16}H_8N_2Na_2O_8S_2$	423/425
		$C_{16}H_8N_2O_8S_2$	210
5-Isatinsulfonic acid sodium salt		$C_8H_4NO_5S \cdot Na$	250

Table 4. Cont.

Compound	Structure	Molecular Formula	MS Fragments (<i>m/z</i>)
Isatin 5-sulfonic acid		C ₈ H ₅ NO ₅ S	228/229
		C ₈ H ₄ NO ₅ S	226/227
		C ₈ H ₆ NO ₆ S	243/244
Isatin		C ₈ H ₅ NO ₂	147
Cyclohexanemethylamine		C ₇ H ₁₅ N	113

4. Materials and Analysis Methods

4.1. Materials

The resins used in this experiment were manufactured by Shaanxi LanShen Special Resin Factory, China. The type of the resin was LS-109D. The resins were pretreated based on the following steps: Firstly, the resin was soaked in the anhydrous ethanol for 24 h and washed with ethanol mixed with water in a volume ratio of 1:5 until the effluent was clear with the absence of ethanol. Secondly, the above resin was soaked in 4% hydrochloric acid for 2 h and washed to neutral with deionized water, and then in 4% sodium hydrate soaked for 2 h and washed to neutral with deionized water. Finally, the resin was dried at 60 °C to constant weight and placed in the dryer for reserve. The initial resin is abbreviated as Virgin. Indigo carmine was purchased from the Sinojpharm Chemical Reagent Co., Ltd. (Shanghai China). The analytical grade of all other reagents was used in the experiment (Aladdin Reagent Co., Ltd. Shanghai China). The concentration of 1000 mg/L stock solutions was made by dissolving indigo carmine powder into deionized water. The adopted concentrations in the adsorption experiment were acquired by diluting the stock solution with deionized water.

4.2. The DBD Regeneration Reaction System

The schematic diagram of DBD regeneration system is shown in Figure 11. It primarily included pulsed power supply, oxygen cylinder, and the regeneration reactor. The schematic diagram of the adsorbent-packed DBD reactor is shown in Figure 12. It was a flat type of DBD reactor. The ground electrode and high voltage electrode of DBD reactor was copper sheet. The discharge electrode was placed onto quartz barrier (80 mm × 30 mm × 2 mm). The discharge gap space between the ground and high voltage electrode was kept at 3 mm. In addition, the flat reactor port filled with quartz wool was to prevent the resin from blowing out by the carrier gas during the discharge process. As the carrier gas of oxygen, the flow rate was 3 L/min. The discharge voltage and current waveforms were recorded with the oscilloscope (Tektronix TDS 2014, Johnston, OH, USA), with a voltage probe (Tektronix P6021, Johnston, OH, USA) and a current probe (Tektronix P6021, Johnston, OH, USA), which are shown in Figure 13. The discharge parameters in the regeneration process were pulse

frequency of 1 kHz, pulse voltage of 16 kV, current of ~ 4.3 A, storage capacitance C_p of 3.8 pF, and reaction time of 5 min, with a high rise time of about 50 ns.

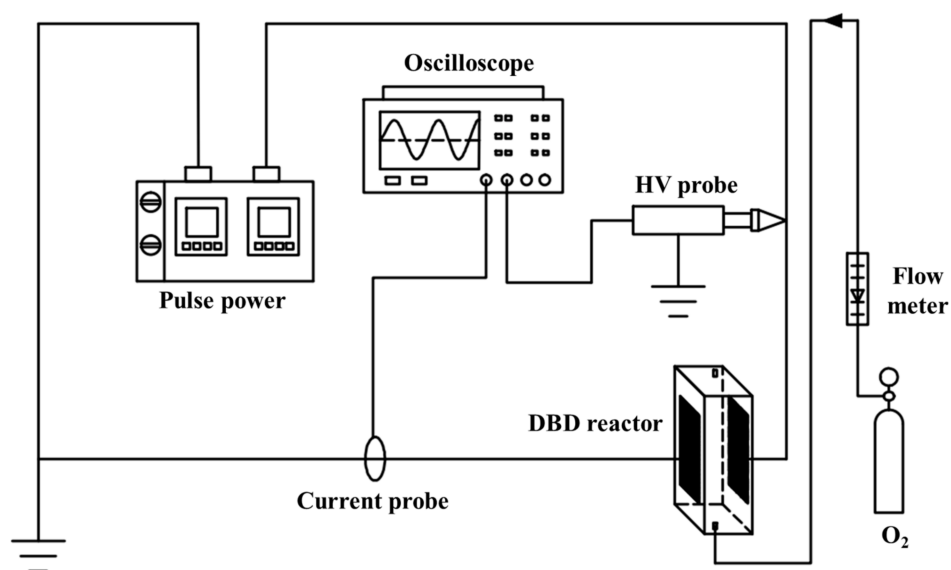


Figure 11. Bench-scale apparatus of DBD plasma for Indigo Carmine decomposition.

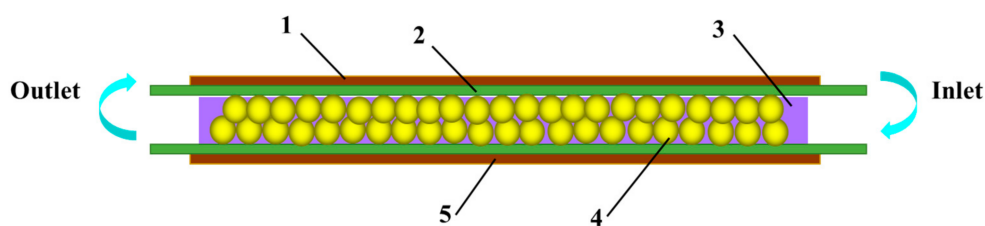


Figure 12. Schematic diagram of the DBD regeneration reactor: 1, high voltage electrode; 2, quartz glass; 3, plasma area; 4, resin; and 5, ground electrode.

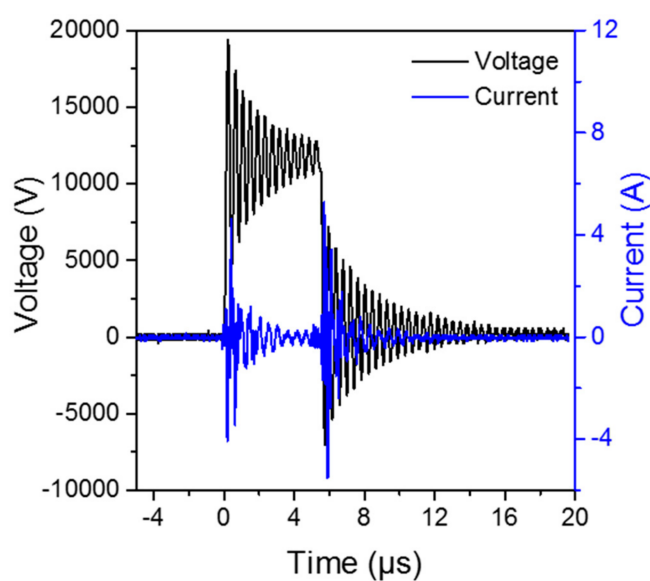


Figure 13. Voltage and current waveforms delivered to the DBD regeneration reactor.

4.3. Analytical Device

The pH of solutions was measured with a FE20 meter (Mettler Toledo, Greifensee, Switzerland). The concentration of indigo carmine was detected by UV-Vis spectrophotometer (Specord® 200 Plus, Analytikjena, Jena, Germany) using the supernatant from the filtered solution and detection at the maximum wavelength of 610 nm. The analytical samples separated from treated solution were filtered with Whatman 0.45 µm PTFE membrane filter before analysis. The intermediates of samples were analyzed by Liquid Chromatograph Mass Spectrometer (Agilent 6400, Agilent Technologies Inc., Santa Clara, CA, USA) analysis with a C18 column and ultraviolet detection at 610 nm. The mobile phase was the volume ratio of 7:3 (*v/v*) between acetonitrile and deionized water (with 0.01% formic acid) with a flow rate of 1 mL/min. Furthermore, the filtrate of samples was extracted thrice with dichloromethane and evaporated in a vacuum evaporator (BUCHI R-300, Buchi, Flawil, Switzerland) with 40 °C water bath, after which a gas chromatography (Agilent 6890N) coupled with a mass selective (Agilent 5975) apparatus and a capillary column (30 mm × 0.25 mm × 0.25 mm) was utilized for identification of byproducts in gas phase during the regeneration process. The functional groups of virgin, saturated and DBD regenerated resin were analyzed by Fourier transform-infrared (FT-IR) spectroscopy. The analytic samples were prepared by mixing 1 mg of the samples with 500 mg of KBr in an agate mortar and scanned in a range from 4000 to 400 cm⁻¹. The structural properties of resin were obtained from the physical adsorption of N₂ at 350 K determined by a Tristar II 3020 equipment. The special surface area was calculated using the BET equation [32]. To evaluate the adsorption capacity, the adsorption equilibrium isotherms of indigo carmine onto resins were measured based on the method provided by Mangun [33].

4.4. The Regeneration of Indigo Carmine Saturated Resin

The regeneration reaction of resins was carried out in the DBD reactor. Before the regeneration process, 0.25 g of saturated resins were put into the reactor. The regeneration reaction started when the power supply was open, which would last for 10 min. The resins were regenerated for five cycles in total. The first to fifth DBD plasma regeneration experiments were abbreviated as DBD1, DBD2, DBD3, DBD4, and DBD5, respectively. During DBD plasma regeneration process, the reaction temperature was not more than 35 °C. All experiments were carried out at atmospheric pressure.

4.5. Kinetics Adsorption

The kinetics adsorption reaction of indigo carmine onto virgin and regenerated resins were operated in oscillatory reactor. The concentration of solution after adsorption was monitored by the mentioned method.

4.6. Adsorption Equilibrium Isotherms

The adsorption isotherms of indigo carmine onto virgin and regenerated resins were operated in oscillatory reactor. Exactly 0.25 g of resins were added into a series of conical bottles containing 100 mL of indigo carmine solution of different concentration. The concentration was 5, 10, 15, 20, 30, 40, 50, 60, 80, and 100 mg/L, respectively. The conical flasks with cover were shaken with a constant speed of 120 rpm at 40 °C for 12 h. Then, the suspension was filtered for further analysis. Based on the standard curves of indigo carmine samples, the concentration was analyzed with UV-Vis spectrophotometer, and the amount of indigo carmine adsorbed onto resins was inferred from Equation (3):

$$q_e = \frac{(C_0 - C_e)V}{m}, \quad (3)$$

where q_e is the amount of indigo carmine adsorbed per gram of resin, mg/g; V is the volume of the liquid phase, L; C_0 is the concentration of the initial solution before it contacts with resin, mg/L; C_e is the concentration of the solution at equilibrium condition, mg/L; and m is the amount of the resin, g.

5. Conclusions

An integrated system of resin adsorption/DBD plasma regeneration method was applied for the degradation of indigo carmine solution. According to the GC-MS and LC-MS analytical results, above 85% of indigo carmine adsorbed on resin was decomposed into sulfonic acid and dehydroxylation byproducts by DBD plasma. Simultaneously, saturated resin was regenerated, and the adsorption capacity of adsorption/DBD plasma regenerated resin could be maintained at a relatively high level after multiple cycles. The functional groups, specific surface area, total pore volume, pore size, and adsorption capacity of regenerated resin did not suffer a large degree of damage. The multiple cycles of regenerative reaction indicated that resin maintained a stable and effective performance for indigo carmine adsorption. Finally, the possible degradation pathway of indigo carmine was proposed in the resin adsorption/DBD plasma regeneration process. This integrated method has a good prospect in the treatment of refractory organic wastewater.

Acknowledgments: The work was supported by Chinese National Nature Science Foundation under Grant 11075041.

Author Contributions: Chunjing Hao conceived, designed and performed the experiments; Zehua Xiao processed the reactor; Di Xu, Chengbo Zhang, Jian Qiu contributed reagents/materials/analysis tools, and Kefu Liu mainly summarized and refined the analysis; and Chunjing Hao wrote the paper.

Conflicts of Interest: The authors declare no conflict of interest.

References

1. Vandevivere, P.C.; Bianchi, R.; Verstraete, W. Treatment and reuse of wastewater from the textile wet-processing industry: Review of emerging technologies. *J. Chem. Technol. Biotechnol.* **1998**, *72*, 289–302. [[CrossRef](#)]
2. Minamitani, Y.; Shoji, S.; Ohba, Y.; Higashiyama, Y. Decomposition of dye in water solution by pulsed power discharge in a water droplet spray. *IEEE Trans. Plasma Sci.* **2008**, *36*, 2586–2591. [[CrossRef](#)]
3. Jiang, S.; Wen, Y.; Liu, K. Treatments of dye wastewater by water spout in the pulsed DBD. In Proceedings of the IEEE International Conference on Plasma Science (ICOPS), Antalya, Turkey, 24–28 May 2015.
4. Khraishah, M.A.M.; Al-Ghouti, M.A.; Allen, S.J.; Ahmad, M.N. Effect of OH and silanol groups in the removal of dyes from aqueous solution using diatomite. *Water Res.* **2005**, *39*, 922–932. [[CrossRef](#)] [[PubMed](#)]
5. Wu, X.; Hui, K.N.; Hui, K.S.; Lee, S.K.; Zhou, W.; Chen, R.; Hwang, D.H.; Cho, Y.R.; Son, Y.G. Adsorption of basic yellow 87 from aqueous solution onto two different mesoporous adsorbents. *Chem. Eng. J.* **2012**, *180*, 91–98. [[CrossRef](#)]
6. Crini, G. Non-conventional low-cost adsorbents for dye removal: A review. *Bioresour. Technol.* **2006**, *97*, 1061–1085. [[CrossRef](#)] [[PubMed](#)]
7. Li, X.Z.; Zhang, M. Decolorization and biodegradability of dyeing wastewater treated by a TiO₂-sensitized photo-oxidation process. *Water Sci. Technol.* **1996**, *34*, 49–55.
8. Azbar, N.; Yonar, T.; Kestioglu, K. Comparison of various advanced oxidation processes and chemical treatment methods for COD and color removal from a polyester and acetate fiber dyeing effluent. *Chemosphere* **2004**, *55*, 35–43. [[CrossRef](#)] [[PubMed](#)]
9. Raghu, S.; Basha, C.A. Chemical or electrochemical techniques, followed by ion exchange, for recycle of textile dye wastewater. *J. Hazard. Mater.* **2007**, *149*, 324–330. [[CrossRef](#)] [[PubMed](#)]
10. Garcia-Montano, J.; Ruiz, N.; Munoz, I.; Domenech, X.; Garcia-Hortal, J.A.; Torrades, F.; Peral, J. Environmental assessment of different photo-Fenton approaches for commercial reactive dye removal. *J. Hazard. Mater.* **2006**, *138*, 218–225. [[CrossRef](#)] [[PubMed](#)]
11. Fongsatitkul, P.; Elefsiniotis, P.; Yamasmit, A.; Yamasmit, N. Use of sequencing batch reactors and Fenton's reagent to treat a wastewater from a textile industry. *Biochem. Eng. J.* **2004**, *21*, 213–220. [[CrossRef](#)]
12. Pouran, S.R.; Aziz, A.R.A.; Daud, W.M.A.W. Review on the main advances in photo-Fenton oxidation system for recalcitrant wastewaters. *J. Ind. Eng. Chem.* **2015**, *21*, 53–69. [[CrossRef](#)]
13. Kogelschatz, U. Dielectric-barrier discharges: Their history, discharge physics, and industrial applications. *Plasma Chem. Plasma Process.* **2003**, *23*, 1–46. [[CrossRef](#)]

14. Clements, J.S.; Sato, M.; Davis, R.H. Preliminary investigation of pre-breakdown phenomena and chemical-reactions using a pulsed high voltage discharge in water. *IEEE Trans. Ind. Appl.* **1987**, *23*, 224–235. [[CrossRef](#)]
15. Eliasson, B.; Kogelschatz, U. Modeling and applications of silent discharge plasmas. *IEEE Trans. Ind. Appl.* **1991**, *19*, 309–323. [[CrossRef](#)]
16. Laroussi, M. Nonthermal decontamination of biological media by atmospheric-pressure plasmas: Review, analysis, and prospects. *IEEE Trans. Plasma Sci.* **2002**, *30*, 1409–1415. [[CrossRef](#)]
17. Vergara Sanchez, J.; Torres Segundo, C.; Montiel Palacios, E.; Gomez Diaz, A.; Reyes Romero, P.G.; Martinez Valencia, H. Degradation of textile dye AB 52 in an aqueous solution by applying a plasma at atmospheric pressure. *IEEE Trans. Plasma Sci.* **2017**, *45*, 479–484. [[CrossRef](#)]
18. Kuroki, T.; Fujioka, T.; Kawabata, R.; Okubo, M.; Yamamoto, T. Regeneration of honeycomb zeolite by nonthermal plasma desorption of toluene. *IEEE Trans. Ind. Appl.* **2009**, *45*, 10–15. [[CrossRef](#)]
19. Jiang, B.; Zheng, J.; Lu, X.; Liu, Q.; Wu, M.; Yan, Z.; Qiu, S.; Xue, Q.; Wei, Z.; Xiao, H.; et al. Degradation of organic dye by pulsed discharge non-thermal plasma technology assisted with modified activated carbon fibers. *Chem. Eng. J.* **2013**, *215*, 969–978. [[CrossRef](#)]
20. Hao, X.L.; Zhang, X.W.; Lei, L.C. Degradation characteristics of toxic contaminant with modified activated carbons in aqueous pulsed discharge plasma process. *Carbon* **2009**, *47*, 153–161. [[CrossRef](#)]
21. Berenguer, R.; Marco-Lozar, J.P.; Quijada, C.; Cazorla-Amoros, D.; Morallon, E. Electrochemical regeneration and porosity recovery of phenol-saturated granular activated carbon in an alkaline medium. *Carbon* **2010**, *48*, 2734–2745. [[CrossRef](#)]
22. Dabrowski, A.; Podkoscielny, P.; Hubicki, Z.; Barczak, M. Adsorption of phenolic compounds by activated carbon—A critical review. *Chemosphere* **2005**, *58*, 1049–1070. [[CrossRef](#)] [[PubMed](#)]
23. Lin, S.; Juang, R. Adsorption of phenol and its derivatives from water using synthetic resins and low-cost natural adsorbents: A review. *J. Environ. Manag.* **2009**, *90*, 1336–1349. [[CrossRef](#)] [[PubMed](#)]
24. Iyim, T.B.; Acar, I.; Oezguemues, S. Removal of basic dyes from aqueous solutions with sulfonated phenol-formaldehyde resin. *J. Appl. Polym. Sci.* **2008**, *109*, 2774–2780. [[CrossRef](#)]
25. Fan, J.; Li, H.; Shuang, C.; Li, W.; Li, A. Dissolved organic matter removal using magnetic anion exchange resin treatment on biological effluent of textile dyeing wastewater. *J. Environ. Sci.* **2014**, *26*, 1567–1574. [[CrossRef](#)] [[PubMed](#)]
26. Wang, C.; Lippincott, L.; Meng, X. Feasibility and kinetics study on the direct bio-regeneration of perchlorate laden anion-exchange resin. *Water Res.* **2008**, *42*, 4619–4628. [[CrossRef](#)] [[PubMed](#)]
27. Foo, K.Y.; Hameed, B.H. Insights into the modeling of adsorption isotherm systems. *Chem. Eng. J.* **2010**, *156*, 2–10. [[CrossRef](#)]
28. Sundaraganesan, N.; Anand, B.; Meganathan, C.; Joshua, B.D. FT-IR, FT-Raman spectra and ab initio HF, DFT vibrational analysis of 2,3-difluoro phenol. *Spectrochim. Acta A* **2007**, *68*, 561–566. [[CrossRef](#)] [[PubMed](#)]
29. Ahmed, M.A.; Brick, A.A.; Mohamed, A.A. An efficient adsorption of indigo carmine dye from aqueous solution on mesoporous Mg/Fe layered double hydroxide nanoparticles prepared by controlled sol-gel route. *Chemosphere* **2017**, *174*, 280–288. [[CrossRef](#)] [[PubMed](#)]
30. Reddy, P.M.K.; Raju, B.R.; Karuppiah, J.; Reddy, E.L.; Subrahmanyam, C. Degradation and mineralization of methylene blue by dielectric barrier discharge non-thermal plasma reactor. *Chem. Eng. J.* **2013**, *217*, 41–47. [[CrossRef](#)]
31. Wang, J.; Lu, L.; Feng, F. Improving the indigo carmine decolorization ability of a bacillus amyloliquefaciens laccase by site-directed mutagenesis. *Catalysts* **2017**, *7*, 275. [[CrossRef](#)]
32. Qu, G.-Z.; Li, J.; Wu, Y.; Li, G.-F.; Li, D. Regeneration of acid orange 7-exhausted granular activated carbon with dielectric barrier discharge plasma. *Chem. Eng. J.* **2009**, *146*, 168–173. [[CrossRef](#)]
33. Mangun, C.L.; Benak, K.R.; Economy, J.; Foster, K.L. Surface chemistry, pore sizes and adsorption properties of activated carbon fibers and precursors treated with ammonia. *Carbon* **2001**, *39*, 1809–1820. [[CrossRef](#)]

